Cement and Concrete Research 42 (2012) 344–357

Contents lists available at SciVerse ScienceDirect

Cement and Concrete Research

journal homepage: http://ees.elsevier.com/CEMCON/default.asp

Water demand of amorphous nano silica and its impact on the workability of cement paste

G. Quercia [a,b,*], G. Hüsken [b], H.J.H. Brouwers [b]

[a] Materials innovation institute (M2i), Mekelweg 2, P.O. Box 5008, 2600 GA Delft, The Netherlands
[b] Eindhoven University of Technology, Department of the Built Environment, P.O. Box 513, 5600 MB Eindhoven, The Netherlands

ARTICLE INFO

Article history:
Received 19 January 2011
Accepted 21 October 2011

Keywords:
Nano silica (D)
Particle size distribution (B)
Surface area (B)
Water demand (A)
Workability (A)

ABSTRACT

This paper addresses the characterization of six different amorphous silica samples with respect to their application in cement paste. Different mixes are compared and analyzed using the mini spread-flow test. Also the granular properties, different void fraction states of packing and distribution moduli q are analyzed and compared using a mix design tool. A deformation coefficient is derived from the spread-flow test, which correlates with the value of specific surface area computed from the particle size distribution, and intrinsic density of the samples. Finally, the thickness of a constant water layer of 25 nm around the particles is computed at the onset of flowing. The granular analysis demonstrated that it is possible to decrease the water demand of the cement paste when nanoparticles are added and the resulting grading follows the modified Andreasen and Andersen curve ($q = 0.5$), and the concentration of nano silica is less than 5% bwoc.

1. Introduction

The construction industry uses concrete to a large extent worldwide. About 14 billion tons were used in 2007 [9]. Concrete is composed of granular materials of different sizes and the size range of the composed solid mix covers a wide interval (Fig. 1). The smallest particle in standard concrete, usually cement, is typically in the range of 300 nm to 90 μm, whereas the largest constituent, gravel, can be up to 32 mm. These particles are composed to produce the concrete mix. The combination of all individual particle size distributions (PSDs) of the raw materials results in an overall PSD of the mix. This overall grading of the mix, containing particles from 300 nm to 32 mm, so 5 orders of magnitude, determines the mix properties of the concrete [33,45]. The properties in fresh state, flow behavior and workability, are for instance governed by the overall grading of the mix, but also the properties of the concrete in hardened state, such as strength and durability, are affected by the mix grading and resulting particle packing [52]. One way to further improve the packing is to increase the solid size range, e.g. by including particles with sizes below 300 nm. Possible materials that are currently available are limestone and silica fines, such as silica sand (SS), micro silica (mS), silica fume (Sf) and nano silica (nS). Nowadays, there are different methods used to produce nS like sol–gel process, vaporization of silica, biological method and precipitation [51]. The main characteristics of silica fines, such as particle size distribution, specific density, specific surface area, and reactivity (surface silanol groups), depend on the production method used [57].

The application of micro silica (mS and Sf) in concrete involves two different mechanisms. The first one is the chemical effect: the pozzolanic reaction of silica (SiO_2) with calcium hydroxide ($Ca(OH)_2$) forms more CSH-gel ($xCaO.ySiO_2.zH_2O$) at final stages. The second function is a physical one, because micro silica is about 100 times smaller than cement. Micro silica can fill the remaining voids in the young and partially hydrated cement paste, increasing its final density [60]. Some researchers [21,60] indicate that the addition of 1 kg of micro silica allows for a reduction of about 4 kg of cement (efficient factor of 3–4 in concrete with w/c less than 0.55), and this effect can be higher if nS is used. Another possibility is to maintain the cement content at a constant level, but optimizing the particle packing by using fine stone wastes in order to obtain a broader PSD [30]. Optimizing the PSD will increase the properties (strength, durability) of the hardened concrete due to a denser granular structure [17,53].

This paper presents, at first instance, a characterization of several commercial amorphous silica samples, and their particle size distribution and specific surface area determined by different techniques are compared. Then an extended analysis of the effects of amorphous silica on the water demand, water film layer derivation and workability of cement paste using the mini spread-flow test is presented. Furthermore, the granulometric properties of the paste are analyzed and relations of the resulting calculated void fraction and distribution modulus q are made using the results obtained by an optimization algorithm developed by Hüsken and Brouwers [33].

* Corresponding author at: Materials innovation institute (M2i), Mekelweg 2, P.O. Box 5008, 2600 GA Delft, The Netherlands.
E-mail address: g.quercia@tue.nl (G. Quercia).

0008-8846/$ – see front matter © 2011 Elsevier Ltd. All rights reserved.
doi:10.1016/j.cemconres.2011.10.008

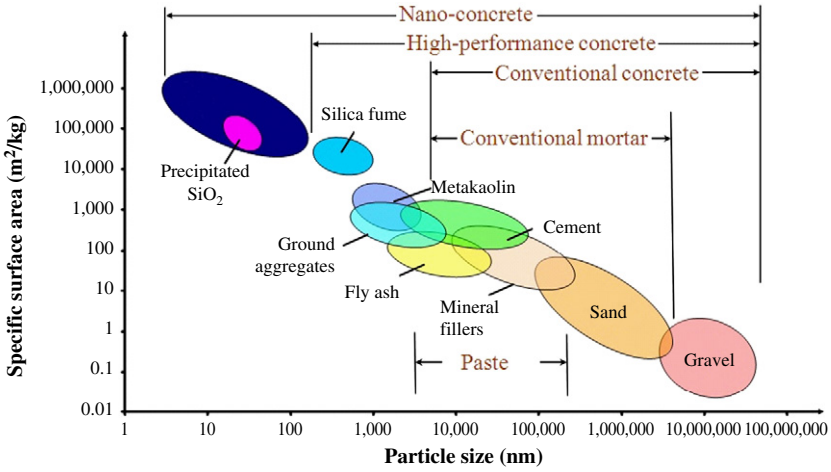

Fig. 1. Size range and specific surface area of concrete ingredients, taken from Sobolev and Ferrada [56].

2. Application of nano silica in cement paste

Nano silica addition in cement paste and concrete can result in different effects. The accelerating effect in cement paste is well reported in the literature [8,39,50,54,55]. The main mechanism of this working principle is related to the high specific surface area of nS, because it works as nucleation site for the precipitation of CSH-gel. However, according to Bjornstrom et al. [4] it has not yet been determined whether the more rapid hydration of cement in the presence of nS is caused by its chemical reactivity upon dissolution (pozzolanic activity) or is related to the considerable surface activity. Nevertheless, Byung-Wan et al. [8] studied the accelerating effect of nS in mortars and they found that this effect is low in the first 22 min, according to their calorimetric curves presented for OPC mortar with 10% of nS. During the first stage of reaction there is an increase in the heat release, and then this heat drops during the beginning of the induction period of hydration. This phenomenon is also presented by Belkowit and Armentrout [6], who found that in the beginning of the calorimeter test a difference of only 4 °F between a reference cement paste and nS pastes with varied particle sizes (8 to 508 nm) was measured. In other words, it was observed that the accelerating effect of nS depends on the source of origin and the production method (colloidal or dry powder). Even though the beneficial effect of nS addition is reported, its concentration is limited to a maximum level of 5% to 10% based on the weight of cement (bwoc), depending on the researcher or reference [51]. At high nS concentrations the autogenous shrinkage due to self-desiccation increases and results, consequently, in a higher cracking potential.

2.1. Effect of nano silica addition on the workability

Recently, the accelerating effect of nS addition was established indirectly by rheological measurements (viscosity change) of cement pastes and mortars [54,55]. The viscosity measurements have shown that cement paste and mortar with nS addition need more water to keep the workability of the mixtures constant. Even though rheometric techniques are more accurate, they can be time-consuming and are often technically difficult to perform compared with standard workability tests, like the mini spread-flow test. Another disadvantage is that cement pastes need to be conditioned at the beginning and stirred to obtain first measurements. This procedure takes normally about 20 min after the initial mixing and is reported by several researchers for rheological studies on nS and mS [23,24,42,54,55,59]. Furthermore, it can be concluded that nS exhibits stronger tendency for adsorption of ionic species in the aqueous medium [2] and the formation of agglomerates is expected.

In contrast to the rheometric measurements, the mini spread-flow test described by Okamura and Ozawa [46], is an efficient and classical technique that is used nowadays by several researchers as a method to determine the water demand of powders and mortars [3,20,32,38,49]. It is suitable in particular for the measurement of materials that have a collapsed slump. In the paste at the onset of flowing, a layer of adsorbed water molecules surrounds the fine particles and an additional amount of water is needed to fill the remaining void fraction of the granular system. Since fine powders provide by far the largest contribution to the total specific surface area, they have also the strongest influence on the total water demand of a concrete mix. As a result, the powders should have a preferably low water demand. Therefore, an appropriate determination of the amount of water, needed to cover all particles with a water layer of a certain thickness, is an important parameter. Brouwers and Radix [5], Hunger and Brouwers [30], and later Hunger [31] found a relationship between the specific surface area and the water demand of micro powder using the mini spread-flow test. They reported a constant water layer of 25 nm for several tested powders. It is interesting to investigate if the same relationship can be found at nanoscale. Several reports can be found in the literature on the effect of nS on the workability of cement paste using rheometric measurements, but the effect on the water demand using the mini spread-flow test has not be reported so far.

2.2. Effect of nanoparticles addition on the granular mix

Hüsken and Brouwers [33] developed an optimization algorithm to design the best grading curve to obtain the maximum packing of a certain granular mix. This new mix design tool is based on the modified Andreasen and Andersen equation suggested by Funk and Dinger [27]. By means of this mix design tool a granular mix is composed based on the ideas of continuous geometric random packing of polydisperse particles. Brouwers and Radix [5] concluded in a previous work that it could be expected that if one would optimize the PSD down in the nanometer range, the workability and stability could be maintained while further reducing the necessary superplasticizer content. In this context, a brief analysis of the developed grading algorithms is also given with the objective to test their applicability for particles at nanoscale.

3. Materials and experimental methods

3.1. Materials

The Portland cement used was CEM I 52.5 N, as classified by [12]. This cement consists to more than 95% by mass of Portland cement

Table 1
Specification and general characteristics of the employed amorphous silica samples and the cement.

Name	CnS-1	CnS-2	PnS-3	PmS-4	PmS-5	PmS-6	Cement
Type	Colloidal	Colloidal	Powder	Slurry	Powder	Powder	CEM I 52.5 N
Specific density (g/cm^3)[a]	1.10	1.39	2.10	1.39	2.05	2.19	3.15
Bulk density (g/cm^3)	1.05[b]	1.40[b]	0.09–0.11[b]	1.40[b]	09–0.11[b]	0.15–0.70[b]	1.96
pH	9–11	9–11	5[c]	5–7	5[c]	5–7[c]	–
Solid content (% w/w)	15[b]	50[b]	–	48–50[b]	–	–	–
Viscosity (mPa.s)	<50[b]	<50[b]	–	–	–	–	–
Loss on ignition (L.O.I.)	–	–	0.5[b]	4[b]	0.5[b]	0.5[b]	2.8
BET (m^2/g)	234	50	56	23	50	12	0.9
Particle sizes range by SEM/STEM (nm)	5–50	19–156	14–187	14–332	23–391	29–658	–
Particle sizes range by LLD/DLS (nm)	0.9–2.3	79–186	73–291	78–1300	194–446	348–12000	275–91000
SSA_{sph} (cm^2/cm^3)10^{-4}	364	46	48	34	22	8	2

[a] Determined according to DIN EN 1097-7 [18].
[b] Values taken from product data sheet.
[c] 4% w/w in water.

clinker; the initial setting time is 45 min, a water demand of 38.9% by weight, and compressive strength of more than 30.0 N/mm^2 for 2 days and more of 52.5 N/mm^2 at 28 days [22] is obtained. Other physical properties are shown in Table 1. Six different commercial silica (amorphous SiO_2 particles) were selected to determine the water demand and to perform the subsequent analysis. These samples are classified and named as follows: two colloidal nano silica suspensions from Akzo Nobel Germany, *Cembinder® 50* and *Cembinder® 8* (samples CnS-1 and CnS-2, respectively); and four micro silica samples provided by Elkem Materials Norway, one nano silica fume, *Submicron silica 995* (PnS-3) in powder form, one standard micro silica fume *(EMSAC® 500S)* in slurry form (PmS-4); and two experimental

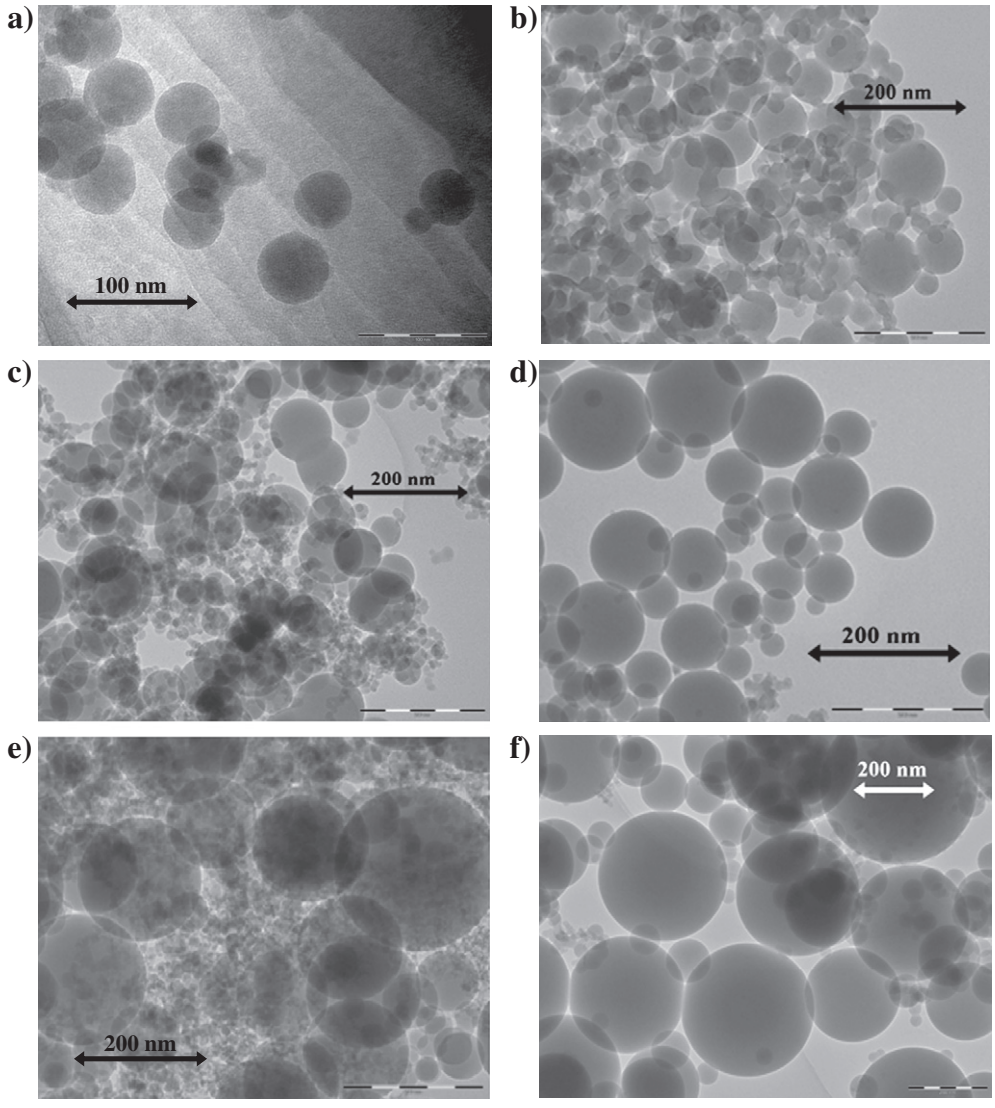

Fig. 2. SEM-photographs of different nS/mS studied: a) CnS-1, b) CnS-2, c) PnS-3, d) PmS-4, e) PmS-5 and f) PmS-6.

synthetic pyrogenic silica samples with different specific BET surface area (PmS-5 and PmS-6). Their general characteristics taken from the product data sheet are shown in Table 1.

3.2. Experimental methods

3.2.1. Particle morphological characteristics

The size and morphology of the silica fines were analyzed with a scanning electron microscope FEI XL-30 SFEG and a scanning transmission electron microscope Tecnai model 20FEG using a Schottky field emitter gun with a voltage between 55 and 175 keV. Furthermore, a general chemical analysis was performed using an EDAX energy dispersive spectroscopy (EDS) device. The results are shown in Table 1 and Fig. 2.

3.2.2. Particle size distribution (PSD) and specific surface area (SSA) of silica

3.2.2.1. Particle size distribution. The measurement of particle size distributions (PSDs) is a major aspect of powder technology. There are numerous methods suitable for determining PSDs, even though, the most used for fine powders are laser light diffraction (LLD) and dynamic light scattering (DLS). LLD was used to determine the PSD of the commercial nS and mS samples. This technique has become the most prevalent method for the characterization of powders in research and industry [13]. With special analysis software, conclusions can be drawn even in regard to the particle shape. All PSDs of the collected silica have been measured in liquid dispersion (water) with a Malvern Mastersizer 2000 using Mie scattering as measuring principle and following the ISO standard 13320-1 [35]. A Hydro S unit was applied as wet dispersing unit [61]. A spherical particle shape was assumed to calculate the PSD and to compute the specific surface area (SSA_{shp}) for all silica samples based on their arithmetic diameter and the procedure described by Hunger [31]. A general angular model was assumed for the cement sample.

Dynamic light scattering (DLS), sometimes referred to as photon correlation spectroscopy (PCS) or quasi-elastic light scattering (QELS), is a non-invasive, well-established technique for measuring the size of molecules and particles typically in the submicron region. The diameter that is measured by DLS is called the hydrodynamic diameter ($D_{(H)}$) and refers to how a particle diffuses within a liquid. The diameter obtained by this technique is the size of a sphere that has the same translational diffusion coefficient as the particle being measured. The translational diffusion coefficient depends not only on the size of the particle "core", but also on the surface structure as well as the concentration and type of ions in the medium. This means that the size can be larger than measured by electron microscopy [36,58]. The PSDs of the two colloidal nano silica (CnS-1 and CnS-2) have been measured in liquid dispersion (water) using a Malvern Zetasizer Nano ZS DLS, according to Ref. [36]. A conventional cell was used for particle size measurement (distribution in volume). The resultant main parameter and the corresponding PSD of the silica fines are shown in Table 1 and are summarized in Fig. 3.

3.2.2.2. Computed specific surface area (SSA_{Sph}). The specific surface area is the quotient of the absolute available surface, inclusive all open internal surfaces (pore walls), divided by the mass and is expressed in area per mass (m^2/g). In this research, only the outer surface being in contact with water is of interest. Considering the specific density (ρ_s), Table 1, the computed spherical specific surface area (SSA_{Sph}) can also be expressed as area per volume (cm^2/cm^3). Besides mass and solid volume, the (SSA_{Sph}) can also be related to the bulk volume (taking account for the void fraction). The (SSA_{Sph}) was derived indirectly from the particle size distribution using the procedure described by McCabe and Smith [43] and later by Hunger [31].

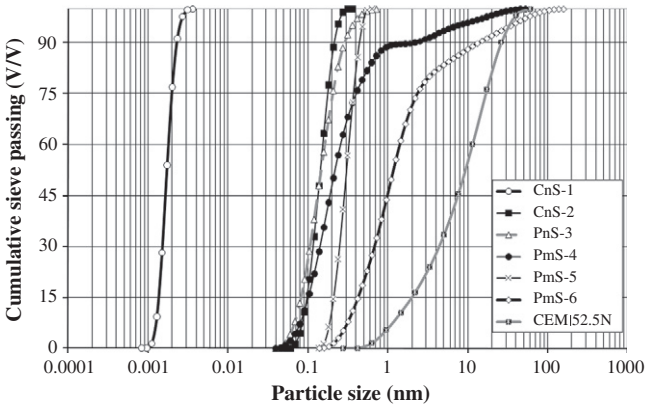

Fig. 3. PSD of the collected nano silica samples and the employed cement (CEM I 52.5 N).

This procedure takes into account the specific density and the measured PSDs to compute the (SSA_{Sph}) of all materials using the following equation:

$$SSA_{Sph} = 6\sum_{i\approx 1}^{n} \frac{w_i}{D_{i,arith}^{i+1}\cdot \rho_s} \quad (1)$$

where (w_i) is the corresponding mass fraction (i), ($D_{i,arith}^{i+1}$) is the arithmetic mean between two consecutive sieve sizes, being the mass percentage of the fraction between (D_i) and (D_{i+1}). The results are show in Table 1.

3.2.2.3. BET specific surface area ($SSA_{BET,total}$ and $SSA_{BET\ ext}$). Gas sorption (both adsorption and desorption) at the clean surface of solid is the most commonly used method for determining the surface area of powders as well as the pore size distribution of porous materials. The specific surface areas of silica samples were analyzed using the Brunauer–Emmet–Teller (BET method) developed in 1938 [7]. The BET analysis is based on the amount of N_2 gas adsorbed at various partial pressures (eight points in the range $0.05<P/P_0<0.3$). A nitrogen molecular cross sectional area of 0.162 nm^2 was used to determine the surface area. Using the BET theory and the standard procedure described by DIN ISO 9277 [19], the specific surface area of the silica samples was determined using a Micromeritics Tristar 3000 adsorption device and calculated from the adsorption/desorption isotherms of N_2.

The nitrogen sorption data were used to compute the micropore volume following the *t*-plot method described by De Boer and Lippens [14]. The statistical thickness of the adsorbed gas layer was also calculated at a given value of (P/P_0) for a nonporous standard adsorbent (standard silica from Micromeritics), using the model proposed by Harkin and Jura [29]. Finally, the external specific surface ($SSA_{BET,\ ext}$) area was determined from the slope of the straight line of the statistical thickness of standard silica sample and the adsorption volume at the pressure range $0.10<P/P_0<0.35$.

3.2.3. Water demand, void fraction and workability of cement/nano silica pastes

Cement pastes with different silica addition were prepared at variable water/powder ratio between 0.5 and 0.7. In total, 97 cement pastes were produced with 0%, 0.5%, 1.5%, 3.0% and 4.5% silica addition based on the weight of cement (bwoc), maintaining a constant weight of 1 kg of cement for each mix (see Table 2). The same procedure used by Ref. [46], and later by Ref. [20] was followed (no use of superplasticizer). A superplasticizer was not used in the present study. The cement pastes were mixed according to EN 196-1 [11] using a 5 l Hobart mixer. The pastes were tested after mixing using the mini spread-flow test applying the Hägermann cone described

Table 2
Analyzed paste formulations.

(wt.%)	w/p	Water (ml)	Cement (g)	Silica fine (g)
0	0.50	500 ± 1	1000	–
	0.55	550 ± 1	1000	–
	0.60	600 ± 1	1000	–
	0.65	650 ± 1	1000	–
	0.70	700 ± 1	1000	–
0.5	0.50	498 ± 1	1000	5
	0.55	548 ± 1	1000	5
	0.60	598 ± 1	1000	5
	0.65	662 ± 1	1000	5
	0.70	701 ± 1	1000	5
1.5	0.50	504 ± 1	1000	15
	0.55	554 ± 1	1000	15
	0.60	604 ± 1	1000	15
	0.65	655 ± 1	1000	15
	0.70	721 ± 1	1000	15
3.0	0.50	510 ± 1	1000	30
	0.55	562 ± 1	1000	30
	0.60	613 ± 1	1000	30
	0.65	665 ± 1	1000	30
	0.70	716 ± 1	1000	30
4.5	0.50	518 ± 1	1000	45
	0.55	570 ± 1	1000	45
	0.60	622 ± 1	1000	45
	0.65	675 ± 1	1000	45
	0.70	727 ± 1	1000	45

in EN 1015-3 [10]. This was done in order to minimize the effect of possible reactivity of the silica fines, assuming that in the first eight minutes no considerable dissolution of the silica fines takes place. The relative slump (Γ_p) was calculated according to Okamura and Ozawa [46] from:

$$\Gamma_p = \left[\frac{\left(\frac{D_1+D_2}{2}\right)}{D_0}\right]^2 - 1 \tag{2}$$

where (D_1) and (D_2) are the spread-flow of the sample measured perpendicular to each other, and (D_0) is the cone base diameter (100 mm). At least three to five mixes with different water (V_w) to powder (V_p) ratio, by volume, were prepared in order to obtain a trend line for the regression analysis. All computed values (Γ_p) were plotted versus the respective (V_w/V_p) ratio and a linear trend line was fitted through the plotted values, reading:

$$\frac{V_w}{V_p} = \beta_p + E_p\Gamma_p \tag{3}$$

where the intersection of the linear function (β_p) represents the slump flow equal to zero, and is referred to as water demand. This value gives the minimum water amount to assure a fluid cement paste. The deformation coefficient (E_p) was also derived from Eq. (3) and represents the slope of the linear regression line. This value indicates the sensitivity of the mix on the water demand for a specified workability, which means that the mix with a lower deformation coefficient shows a bigger change in deformability to a certain change in the water amount [31].

Taking into account a linear relation and the work of Domone and Hsi-Wen [20], the deformation coefficient of the pure silica fines was calculated using the following equation:

$$E_{p,mix} = f_1 \cdot E_{p,CEMI} + f_2 \cdot E_{p,nS} \tag{4}$$

where f_1 and f_2 are the volume fractions or concentrations in the mix of cement and silica fines respectively. Knowing the deformation coefficient of cement ($E_{p,CEMI}$), ($E_{p,nS}$) of the nano silica can be derived indirectly. Furthermore, the void fraction (ψ) was calculated using the water demand ($\beta_{p,mix}$) according to the equation given by Brouwers and Radix [5]:

$$\Psi(\Gamma = 0) = \frac{V_w}{V_{total}} = \frac{V_w}{V_w + {}^wV_s} = \frac{\beta_p}{\beta_p + 1} \tag{5}$$

In which (V_w), (V_s) and (V_{total}) are the volume of water, solids as well as the total volume of the mix, respectively, and (β_p) is the interception of the spread-flow line with the abscissa when the relative slump equals to zero.

3.2.4. Derivation of water layer thickness

A thin layer of adsorbed water molecules around the particles is necessary to assure the fluidity of the hydrating system. Brouwers and Radix [5] proposed that the thickness (δ) of this layer is related to the deformation coefficient and the surface area of the material used, which was later confirmed by Hunger [31]. This relation reads:

$$E_{p,nS} = \xi \cdot \delta \cdot SSA_{Sph} \tag{6}$$

where (ξ) is the shape factor and (SSA_{Sph}) is the specific surface area computed from the PSD. Using the different computed (SSA_{Sph}), ($SSA_{BET,\ total}$), ($SSA_{BET,ext}$) and the calculated deformation coefficient, a water film thickness of the nano silica was derived from the slope of a linear regression using Eq. (6) and assuming a shape factor (ξ) of 1. Finally, the different water film layers were compared in the present study.

3.2.5. Particles grading and determination of distribution modulus for cement/silica pastes

The particle grading and the distribution modulus (q) of the granular mix consisting of amorphous silica (nS or mS) and cement particles were calculated based on the optimization algorithm developed by Hüsken and Brouwers [33]. This algorithm is based on the modified Andreasen and Andersen equation proposed by Funk and Dinger [27], which reads as follows:

$$P'(D) = \frac{D^q - D^q_{\min}}{D^q_{\max} - D^q_{\min}}. \tag{7}$$

The previous equation describes the grading of continuously graded formulation of particles considering a minimum (D_{min}) and maximum (D_{max}) size of the particles that are present in the mix. Hence, an aimed composition of the granular mix considering the grading line given by Eq. (7) can result in a paste that meets the minimum void content and, in consequence, minimum water demand (Fig. 4). The algorithm considers (m) ingredients ($k = 1, 2, \ldots, m$), including the non-solid ingredients air and water. For the mix analysis using

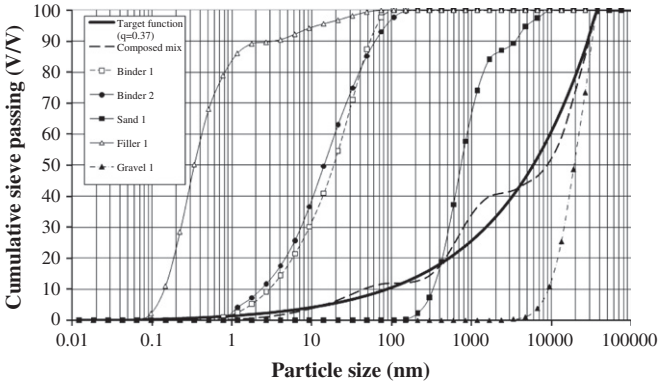

Fig. 4. Example of target line and composed mix derived from the optimization algorithm for cement paste.

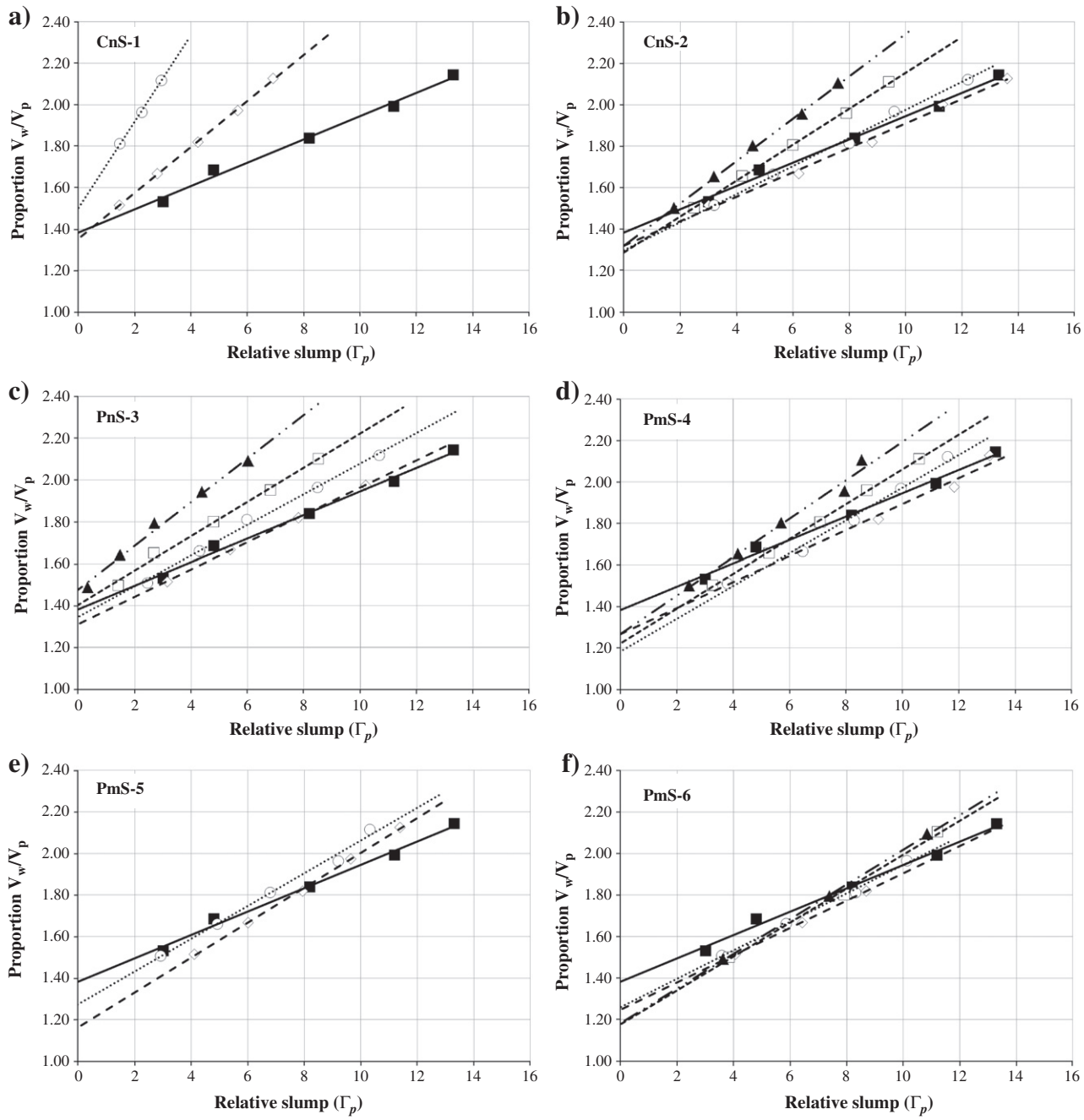

Fig. 5. Variation of water/powder ratio as function of the relative slump flow of cement paste with different addition of nS/mS (◊ 0.5%, ○ 1.5%, □ 3.0% and ▲ 4.5%) based on weight of cement (■), a) CnS-1, b) CnS-2, c), PnS-3, d) PmS-4, e) PmS-5 and f) PmS-6.

Eq. (7), the geometric mean ($D^{i+1}_{i,\,geom.}$) of the upper and lower sieve size of the respective fraction obtained by laser diffraction analysis was taken as particle size (D) and follows from:

$$D^{i+1}_{i,geom.} = \sqrt{D_i \cdot D_{i+1}} \text{ for} i = 1, 2, \ldots, n. \tag{8}$$

The sizes of the fractions vary in steps of √2 starting from 0.01 μm up to 125 mm. Consequently, 44 sizes ($i = 1, 2, \ldots, n+1$) were identified, and 43 fractions (n) are available for the classification of the solid ingredients. Taking this wide range of the PSD of the granular ingredients into account, the entire grading of both materials was considered to obtain a theoretically optimized mix for maximum packing. Using the physical properties of the solids, such as specific density (ρ_s), surface area (SSA_{Sph}), and their PSDs, a grading line (cumulative finer fraction) of the target function was generated on volume base, given by:

$$P_{mix}\left(D^{i+1}_{i,geom.}\right) = P_{mix}\left(D^{i+1}_{i,geom.}\right) - Q_{mix}(D_i), \text{ for } i = 1, 2, \ldots, n-1 \text{or} \tag{9}$$

$$P_{mix}\left(D^{i+1}_{i,geom.}\right) = 1, \text{ for } i = n \tag{10}$$

where Q_{mix} is equal to:

$$Q_{mix}(D_i) = \frac{\sum_{k=1}^{m-2} \frac{v_{sol,k}}{\rho_{s,k}} Q_{sol,k}(D_i)}{\sum_{i=1}^{n} \sum_{k=1}^{m-2} \frac{v_{sol,k}}{\rho_{s,k}} Q_{sol,k}(D_i)}. \tag{11}$$

Using the resulting PSD of the tested mixes, the distribution modulus (q) was assessed using the least squares technique. The

distribution modulus of Eq. (7) was related to the workability properties of the tested pastes. For the analysis, the optimum content of amorphous silica and cement was also calculated using the optimization algorithm. In this case, the distribution modulus (q) varies between 0.01 and 0.50, considering a (w/c) ratio of 0.5 as constraint.

4. Results and discussion

4.1. Morphology, particle size distribution (PSD) and specific surface area (SSA)

The results presented in Table 1 illustrate that the selected silica samples are characterized by diverse PSDs that vary between 2 nm and 12 μm. In general, the particle size distribution determined by STEM measurements is similar compared to DLS and LLD results. In the same way, PSDs are in line with the specific surface area calculated using the BET method, and computed PSDs assuming a spherical shape. However, there is still a need to improve the dispensability of nano silica in water suspensions to obtain the best approximation of the particle size measured by SEM/STEM photomicrographs. It is noteworthy to mention that for the sample CnS-1, only particles of around 20 to 40 nm were identified by electron microscopy. Even though these particles are present in the colloidal suspension, their concentration is less than 2%. For this reason, the DLS results show only particles between 0.09 and 3 nm. These small particles were difficult to identify by the electron microscope used.

The characteristic morphology and shape of all silica samples are presented in Fig. 2. For all nano and micro silica samples studied, a spherical shape is the predominant morphology that was observed. This morphology changes to more angular particles when their particle size becomes smaller than 20 nm. Other observations of the STEM analysis are the evidence of sintered particles (irreversibly agglomerated). The agglomeration of these particles is the result of the high temperature during the collection of silica fume in dust cyclones. In addition, coalesce of particles was also evident in the CnS-2 sample.

Similarly, SEM/STEM analysis revealed that all particles are amorphous with one exception. The sample PmS-4, which is standard micro silica in slurry form, featured small quantities of remnant crystalline faces (detected by electron diffraction spectrum). Probably, these remnants are mainly composed of crystalline SiO_2 and other minor contaminants (Fe, Ca and P), normally found in standard silica fume, and reported by others [25,49].

EDS analysis was performed to identify the main elements that are present in the commercial silica samples, which are in most of the cases silicon and oxygen. In the standard micro silica (PmS-4), iron, calcium and phosphor were identified as impurities. In this case, these elements are possibly resulting from the stabilization additive used for silica slurries that are mainly composed of substances containing phosphates.

4.2. Mini spread-flow test

4.2.1. Water demand analysis

The relative slump flow value of cement–silica mixes versus the volumetric water powder ratio (V_w/V_p) is depicted in Fig. 5a to f for different types and contents of silica. The data illustrate the direct relation between the water demand and the workability of the hydrating system containing amorphous silica and cement. A list of different ($E_{p,mix}$) and ($\beta_{p,mix}$) coefficient found for cement/silica pastes is presented in Table 3. It is important to notice that additions of sample CnS-1 greater than 1.5% bwoc resulted in a too stiff paste. This as a consequence of the increase in the internal surface area that produced higher cohesive forces between the particles. Consequently, it was not possible to measure the spread-flow for the sample CnS-1. In general, the results shown in Table 3 are in line with the theories presented by Brouwers and Radix [5] where ($E_{p,mix}$) depends on the total specific surface area of the solids of the composed mix, which are in the considered case, cement and amorphous silica (nS and mS). It is evident that decreasing particle size of the amorphous silica and, consequently, increasing (SSA), increases the values of ($E_{p,mix}$) for all tested samples. Furthermore, it is clear that the values of the deformation coefficient ($E_{p,mix}$) also increase when the relative concentration of the amorphous silica is higher. However, the water demand also depends on the packing and void fraction of the paste, which explains the minima observed in Fig. 6b to e. In case of improved packing, more water is available to lubricate the particles [5,31], which results in a larger slump flow diameter. Consequently, some values of the water retention ratio ($\beta_{p,mix}$) obtained for mixes with silica addition are lower than the pure cement paste ($\beta_{p,CEMI} = 1.383$).

4.2.2. Void fraction and workability

In order to analyze the results and to unify the effect of the parameters of the spread-flow tests ($E_{p,mix}$ and $\beta_{p,mix}$), the void fraction (ψ) of each mix was calculated from its ($\beta_{p,mix}$) value using Eq. (5). The calculated void fractions were compared with the theoretical water demand (V_w/V_p) necessary for each paste formulation to obtain a relative slump (Γ_p) of 5.3, which is equivalent to a flow diameter of 250 mm. This value is considered as optimum for obtaining good workability in pure cement paste and was indicated by Hunger [31] for cement type I (CEM I 52.5 N). The results obtained for the six selected silica samples and the reference cement are illustrated in Fig. 6a to f. Analyzing these figures it can be concluded that it is possible to reduce the void fraction of the cement paste with 0.5% bwoc of CnS-1. Nevertheless, due to increasing values of the deformation coefficient (E_p), 15% more water is required to obtain a 250 mm slump diameter. Hence, a superplasticizer is needed to reduce the water demand. The higher water demand is caused by the large difference between the specific surface area of CnS-1 (364×10^4 cm^2/cm^3), compared with CEM I 52.5 N (2×10^4 cm^2/cm^3).

For the other colloidal nano silica studied (CnS-2), the reduced void fraction comes along with a reduction in the water demand. This finding is in line with the theories of improved particle packing of continuously graded mixes [1,5,26–28,30,31,33,37,48]. Nevertheless, the minimum void fraction derived from the theoretical analysis is not in line with the point of minimum water demand (Fig. 6b). It means that another mechanism probably exists that is acting in the

Table 3
Computed (E_p) and (β_p) coefficients for cement pastes with different amorphous silica additions, and varying concentrations.

Name	Concentration (% bwoc)	Deformation coefficient ($E_{p,mix}$)	Water demand ($\beta_{p,mix}$)
CEM I 52.5 N	–	0.0562	1.383
CnS-1	0.5	0.1110	1.353
	1.5	0.2084	1.501
CnS-2	0.5	0.0591	1.320
	1.5	0.0677	1.298
	3.0	0.0867	1.288
	4.5	0.1024	1.318
PnS-3	0.5	0.0651	1.312
	1.5	0.0733	1.347
	3.0	0.0821	1.407
	4.5	0.1046	1.481
PmS-4	0.5	0.0568	1.303
	1.5	0.0789	1.184
	3.0	0.0837	1.223
	4.5	0.0925	1.267
PmS-5	0.5	0.0840	1.163
	1.5	0.0787	1.274
PmS-6	0.5	0.0658	1.247
	1.5	0.0685	1.260
	3.0	0.0817	1.178
	4.5	0.0834	1.184

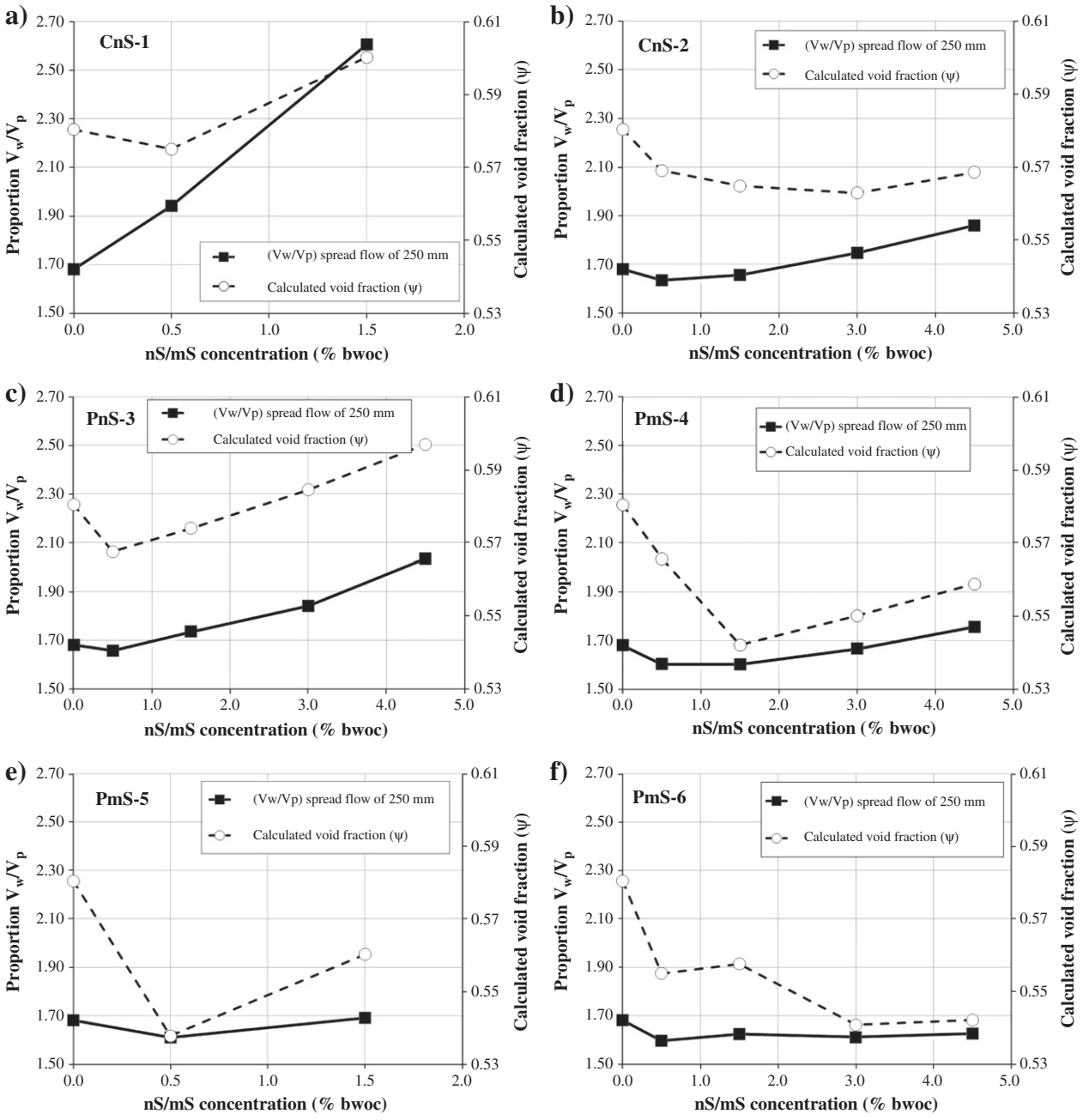

Fig. 6. Theoretical water/powder proportion for a slump flow of 250 mm (■) and calculated void fraction (○) for cement pastes with different addition of nS/mS.

mix, and which modifies the particle packing. Similar phenomena have already been reported by Palm and Wolter [47] as main problem of the application of particles with high specific surface area, i.e. particles in the nanometric range. At nanoscale level, other interparticle forces such as Van der Waals forces, electrostatic repulsion and attraction influence the particle packing. Several researchers [47,62], reported that nanoparticles exhibit lower packing fractions than similar particles with the same composition but with a larger particle size. In contrast to this, it can be noticed from Fig. 6b that it is possible to reduce the water demand of the cement paste by 3%, when CnS-2 is added with a concentration below 2% bwoc. For both mentioned colloidal nano silica samples competing effects between packing behavior and interparticle forces show an important influence on the void fraction and the water demand computed using the spread-flow test. Similar trends in computed (ψ) and (β_p) values were also found for the samples PnS-3 and PmS-5, which reduce the water demand in small additions, maximum 0.9% for PnS-3 and 1.5% bwoc for PmS-5, respectively. It is important to remark that PmS-5 at low concentrations (less than 1.5%) reduces the water demand significantly (5% less water by volume is needed to obtain a flow value of 250 mm).

On the contrary, PmS-4 shows a minimum water demand when a minimum void fraction is obtained (see Fig. 6d). The reduction in the water demand is around 4.5% in volume for an addition of 1.5% bwoc. Moreover, it is possible to obtain a cement paste with the same water demand with an addition of about 3.4% bwoc. This is in line with other work found in the literature, where a reduction of the water demand is reported for a concentration of less than 5% bwoc [54]. However, it is still remarkable that the effect on the reduced water demand due to the incorporation of particles, which result in an

increase in the specific surface area, is extensive. This effect increases the water demand of cement paste with additions larger than 3% of sample PmS-4.

Opposite to other samples, PmS-6 (Fig. 6f) shows a water demand reduction and a minimum void fraction in the entire range of concentrations studied (0.5 to 4.5% bwoc addition). This synthetic pyrogenic silica sample shows a wide PSD that apparently improves the packing of the paste when it is combined with CEM I 52.5 N, as this sample has only four times more SSA than the applied cement, its influence on the packing fraction and the water demand is less. In this case, the spherical shape of the particles results in a rolling effect that reduces the viscosity of the paste. PmS-6 consists of coarse spherical silica that is less reactive than the smaller sized silica and that has a high concentration of nanoparticles. The before mentioned rolling effect is similar to the effect of fly ash [44]. It improves or facilitates the flowing of the cement paste, resulting in a lower water demand to obtain the same slump diameter. As a result, the average water demand was reduced by 5% for all the mixes studied.

In general, the water demand to obtain a slump diameter of 250 mm increases with decreasing particle sizes. Furthermore, the water demand increases when higher silica concentrations are used as illustrated in Fig. 7. One exception of this observation is the sample CnS-1 which has a higher specific surface area than the other samples.

It is also important to notice that the application technique of the silica (suspension, powder, or slurry) can have an effect on the test results. The dispersion of the particles can affect the workability of the mix and, consequently, the packing and the void fraction. To minimize this effect, all samples were first mixed with water and then added to the mixing water before the cement was added. This procedure was suggested by Marchuk [41] as appropriate method for the dispersion of micro silica when a conventional orbital type mixer is used. Even thought this method could not be sufficient to totally disperse the dry amorphous silica powders (PnS-3 and PmS-5), and could be the explanation why, in some cases, the minimum void fraction did not follow the minimum water content. Also, the initial pH value of the pore solution at early ages can be different from amorphous silica introduced in colloidal (CnS-1 and CnS-2) or in slurry form (PmS-4), when both samples are compared with silica in powder form. This fact might explain why the water demand of PnS-3 is higher than that of sample CnS-2 although both samples have similar specific surface area and average particles sizes. In spite of this difference in the water demand, the use of a relative high (V_w/V_p) in the range of 0.5 to 0.7, was chosen to minimize this effect. A further solution can be found by the use of a superplasticizer, which will be considered in the further research.

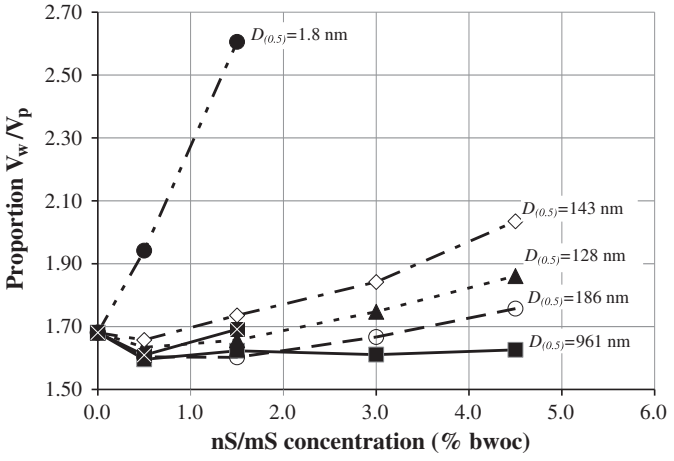

Fig. 7. Theoretical water/powder ratio for a slump flow of 250 mm for cement pastes with different addition and sizes of nano and micro silica (● CnS-1, ◊ PnS-3, ▲ CnS-2, ○ PmS-4 and ■ PmS-6). $D_{(0.5)}$ is the characteristic diameter, where 50% of the particle, by volume, are below in the cumulative finer curves presented in Fig. 3.

Table 4
Estimated volume-based parameters of the spread-flow test of the selected amorphous silica samples.

Name	Deformation coefficient ($E_{p,S}$)
CnS-1	9.0398
CnS-2	0.8947
PnS-3	0.9346
PmS-4	0.7150
PmS-5	1.5562
PmS-6	0.5058

5. Water layer thickness analysis

In the following, the derivation of the water film thickness from the spread-flow tests is described and analyzed. It is important to understand how the different (E_p) values were obtained and their relation to the physical characteristics of the pure nS/mS. The deformation coefficients (E_p) were derived from Eq. (4) and taking into account a linear relation as described by Domone and Hsi-Wen [20]. Considering the respective fraction or concentration of cement and silica in the paste, each ($E_{p,S}$) was calculated indirectly and its derivation is illustrated in Table 4.

Higher deformation coefficients ($E_{p,S}$) were found for mixes with a high content of nano silica (0.935 to 9.040), which is bigger than that of cement (0.0562). This indicates that water has a large influence on the workability of the hydrating system containing nano silica. The results are directly related to the high specific surface area as previously reported by Brouwers and Radix [5] and later by Hunger [31]. These researchers concluded that the larger the external surface, the larger the deformation coefficient (more water is required to attain a certain relative slump). As it is shown in Fig. 8, the present study confirms the relation between the deformation coefficient (E_p) and the specific surface area (SSA_{Sph}) calculated by LLD and DLS.

On the other hand, using the computed (SSA_{Sph}) and the calculated deformation coefficient, a water film having a thickness of 24.8 nm was derived for the silica samples using Eq. (6), (slope value of the linear fit presented in Fig. 8). This value is in the same order of magnitude as the results reported by Brouwers and Radix [5] of 41.3 nm (δ_{Blaine}). Furthermore, this value is also confirmed by Hunger [31], who reported a 24.9 nm based on SSA_{Sph} and 41.6 nm SSA_{Blaine} respectively, for different powders and binders. Moreover, similar values were reported by Marquardt [40], who found a layer thickness of

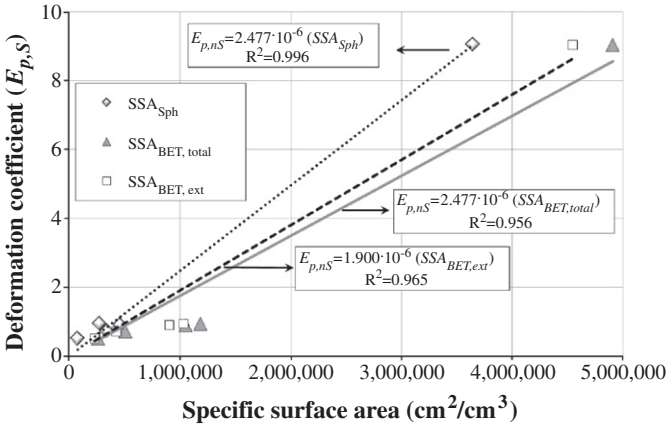

Fig. 8. Computed (SSA_{Sph}) and BET volume based (SSA_{BET}) specific surface area against respective deformation coefficient ($E_{p,S}$) for different silica derived from spread-flow tests.

about 150 water molecules for particles by means of sorption experiments. This layer thickness corresponds to approximately 45 nm as the size of one water molecule is about 3 Å. As the computed specific surface area depends on the efficient dispersion and the primary agglomerated nanoparticles, a similar approach as performed before was carried out using the BET specific surface area (SSA_{BET}). In this case, all (E_p) were plotted against the total and external BET specific surface area (calculated by *t*-plot), and multiplied by the corresponding specific density. In this case, a shape factor is not necessary for correction, because the total BET surface area considers the entire accessible particle surface, including pores. As the surface of the pores is included in the calculation of the water film thickness, the BET external surface area becomes more important. The result is shown in Fig. 8, where the computed water film thickness decreases from 24.8 nm to 19.0 nm, considering only the external surface area ($\delta_{BET,\ ext}$); and from 24.8 nm to 17.4 nm, taking into account the surface area of the pores ($\delta_{BET,\ total}$), respectively. Next, the computed specific surface area (SSA) calculated by LLD or DLS was plotted against ($SSA_{BET,total}$) and ($SSA_{BET,ext}$), see Fig. 9. It is shown that the empirical relation between (SSA_{sph}) and (SSA_{BET}) is linear with a conversion factor in the range of 0.70 to 0.77 for BET total and BET external surface area.

As previously discussed, the application technique of the silica can affect the packing and the workability. Also, the reactivity of the particles has a great influence on the hydration. Nevertheless, the values obtained for the water film layer of all types of amorphous silica with spherical form can partially validate the use of the spread-flow test to calculate the water demand of amorphous nano silica.

The reactivity of the small particles, and a possible effect of the method of incorporation, are minimized by the use of a high water content, the mixing procedure described by Marchuck (1994), and the short time to obtain the spread-flow. At an early stage, the increasing number of contact points and the interlocking of the granular system determine the main mechanisms. The water retention ratio of the nanoparticles influences also the flow properties (nanoparticles apparently need the same water layer thickness as micro particles to obtain the same flow diameter). This phenomenon explains why nano silica is used as stabilization agent in SCC and as anti free water additive in well cementing slurries. Again, a 24.8 nm thick water layer was found in the present research. A similar value was reported by Hunger [31] for micro powders. Both values confirm the applied method and experimental conditions.

6. Particle grading and determination of distribution modulus of cement/silica pastes

The distribution moduli (q) found for mixes of nS/mS and cement particles are listed in Table 5 and vary between 0.56 and 0.20. This

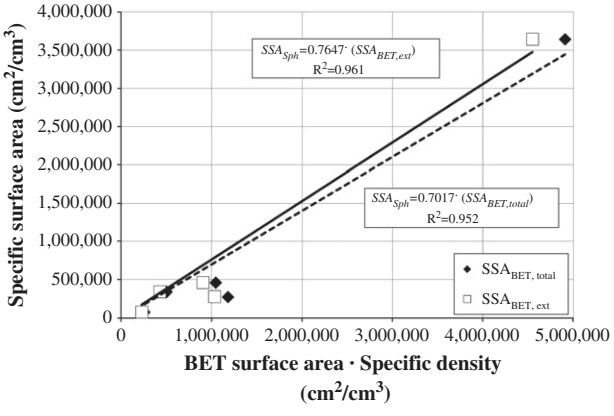

Fig. 9. Linear relation between computed (SSA_{Sph}) and volume based BET (SSA_{BET}) specific surface area.

Table 5
Fitted distribution modulus (q) of cement pastes with addition of amorphous silica.

Name	Concentration (% bwoc)	Distribution modulus (q)	Regression coefficient (R^2)
CnS-2	0.5	0.55	0.9914
	1.5	0.53	0.9928
	3.0	0.50	0.9945
	4.5	0.47	0.9957
PnS-3	0.5	0.55	0.9916
	1.5	0.54	0.9929
	3.0	0.51	0.9945
	4.5	0.48	0.9957
PmS-4	0.5	0.56	0.9914
	1.5	0.54	0.9925
	3.0	0.52	0.9939
	4.5	0.49	0.9950
PmS-5	0.5	0.56	0.9918
	1.5	0.54	0.9928
PmS-6	0.5	0.22	0.9247
	1.5	0.22	0.9264
	3.0	0.21	0.9288
	4.5	0.20	0.9310

variation depends on the overall PSD of each mix. For CnS-2, the minimum void fraction and water demand corresponds to a distribution modulus (q) of 0.5, which is in line with the fixed value postulated by Fuller and Thompson [26], see Fig. 10a. To understand this finding, it is important to analyze the cement grading in detail. The minimum and maximum particle sizes of the cement were used to construct an ideal Fuller type curve. It is evident from Fig. 10 that the cement does not follow the original Fuller curve with (q) of 0.5, because it is deficient of fine particles less than 10 μm. When CnS-2 is added to cement at a maximum ratio of about 3% bwoc, the grading of the composed granular mix is close to the theoretical Fuller curve using Eq. (7), resulting in the maximum packing fraction (lowest void fraction). In the same way, comparing a target curve with (q) of 0.55, a composed mix with 3% bwoc of CnS-2 follows the true Fuller curve for cement. This fact illustrates that the addition of CnS-2 produces a wider particle size distribution of the composed mix, which several researchers reported as a requirement to obtain minimum void fraction (maximum packing), and less water demand [1,26,28,48].

In the same way, all silica samples were analyzed as shown in Fig. 10b to e. For PnS-3, a minimum void fraction and water demand was determined for additions between 0.5 and 1.5% bwoc, which corresponds to (q) values between 0.55 and 0.54. Considering the best fit value (taken from Table 5), which corresponds to a distribution modulus (q) of 0.54, an optimum addition of 3.15% bwoc of PnS-3 was computed from the optimum theoretical grading line. The previous value is close to a distribution modulus of 0.5, which again is the referred value for maximum packing [26]. Even though a difference between the theoretical and calculated distribution modulus exits, the relative concentration of the nS changes, which is caused by introduced errors in the computation of the real PSD as well as the presence of high interparticle forces. These prevent the particles to be arranged in the maximum possible packing. Consequently, the same observation can be made for sample PmS-4, where the minimum water demand was derived for an addition of 1.5% bwoc ($q = 0.54$). This value of (q) corresponds to 4.15% bwoc of PmS-4, which is in line with the calculated values (0.52 for 3% bwoc and 0.49 for 4.5% bwoc) that are, again, close to ($q = 0.5$).

In the case of PmS-5, it was not possible to complete the analysis, as the amount of provided material was not sufficient. Therefore, only two concentrations (0.5 and 1.5% bwoc) were investigated using the mini spread-flow test. However, the difference between the fitted distribution modulus and the computed optimum concentration follows the same trend as explained before. A distribution modulus (q) of

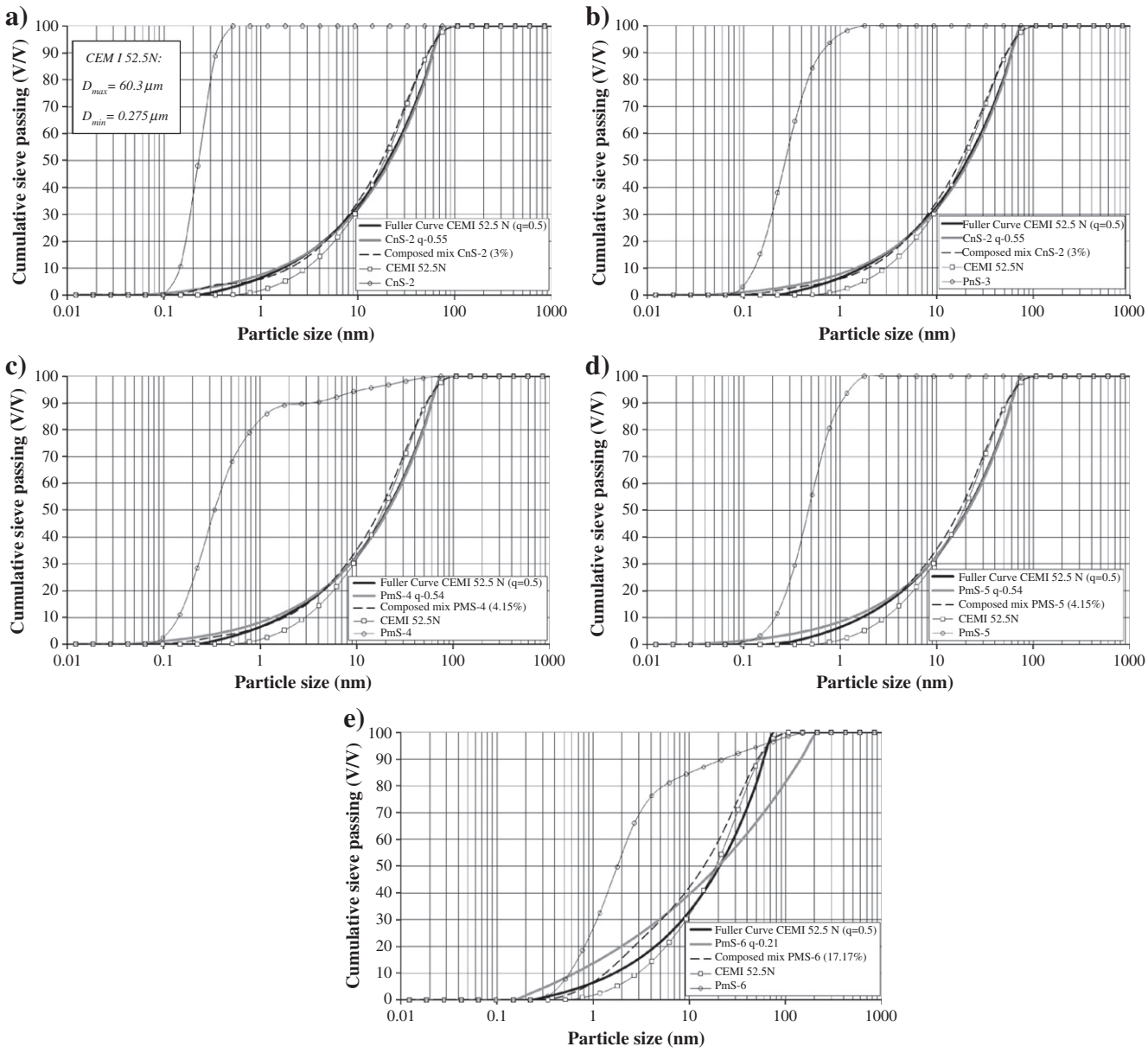

Fig. 10. (a) Target line and composed mix using the optimization algorithm for cement paste with CnS-2 (3% bwoc), and considering the best distribution modulus presented in Table 5 ($q=0.55$, $D_{min}=0.079$ μm, and $D_{max}=60.3$ μm).(b) Target line and composed mix computed using the optimization algorithm for cement paste with PnS-3 (3.5% bwoc), and considering the best distribution modulus presented in Table 5 ($q=0.55$, $D_{min}=0.079$ μm, and $D_{max}=60.3$ μm).(c) Target line and composed mix computed using the optimization algorithm for cement paste with PmS-4 (4.15% bwoc), and considering the best distribution modulus presented in Table 5 ($q=0.54$, $D_{min}=0.053$ μm, and $D_{max}=60.3$ μm).(d) Target line and composed mix computed using the optimization algorithm for cement paste with PmS-5 (3.88% bwoc), and considering the best distribution modulus presented in Table 5 ($q=0.54$, $D_{min}=0.035$ μm, and $D_{max}=60.3$ μm).(e) Target line and composed mix computed using the optimization algorithm for cement paste with PmS-6 (17.17% bwoc), and considering the best distribution modulus presented in Table 5 ($q=0.21$, $D_{min}=0.182$ μm, and $D_{max}=180.0$ μm).

0.54 corresponds to 3.88% bwoc of PmS-5 addition. In practice this 3.88% can be related to a fitted (q) value of about 0.5.

In the case of the PmS-6, the results were completely different to the previously tested samples. In the entire interval of investigated concentrations, the void fraction decreased and the water demand showed a constant value (Fig. 6f). Also, the fitted distribution modulus (q) varied between 0.20 and 0.22. Taking a distribution modulus of ($q=0.2$) into account, an optimum concentration of 17.17% bwoc was computed for this sample. It was not possible to follow the original Fuller curve with the PSD of PmS-6, because this sample contains coarser particles than the cement used. In other words, the particle shape of these coarser particles has also an influence on the spread-flow test that was used to compute the water demand. Furthermore, this type of silica presented a rolling effect that improved the workability of the paste and influenced the final results. Nevertheless, the finding is in line with the distribution modulus used for self compacting concrete (SCC) found by Hunger [31], who reported an ideal range between 0.20 and 0.25 for this type of mixes with high fine content. At the same time, the theories of "filling gap materials" can be used to explain the results [15,16,47]. Some researchers found for mixes of granular materials with a large difference in their average particle size, that it is possible to achieve maximum packing and, consequently, a minimum void fraction. This effect becomes predominant for a difference in the size ratio larger than ten [53]. Here, the average particle size of cement is around 10 μm and the average particle size of the PmS-6 sample is around 1 μm (0.961 nm). Apparently, this size ratio contributes to the reduction of the water demand for all concentrations that were studied in this research (0.5 to 4.5% bwoc).

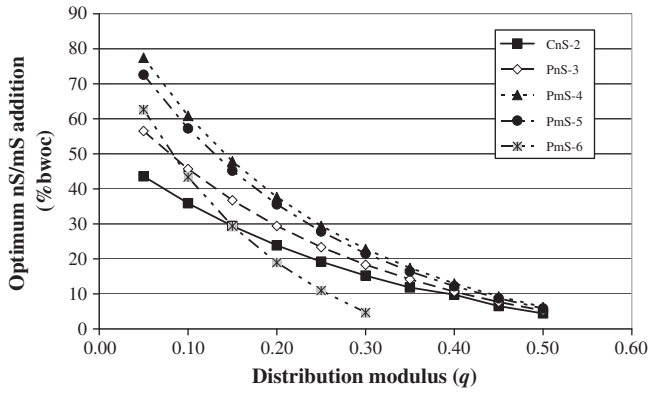

Fig. 11. Relation between the computed additions of different nS/mS (% bwoc) for maximum packing derived from the optimization algorithm of Hüsken and Brouwers [33] and the selected distribution moduli (q).

6.1. Sensitivity analysis of the optimization algorithm

In addition to the grading analysis presented before, a sensitivity study using the optimization algorithm developed by Hüsken and Brouwers [33] was performed to validate the suitability of the algorithm when nano-sized particles are added to the cement paste and mortar. For this analysis, the PSDs of six selected amorphous silica were used to calculate the optimum concentration varying the distribution modulus (q) between 0.05 and 0.50. The results are shown in Fig. 11, where, in general, the concentration of fine material increases with decreasing distribution modulus (q). This fact was expected and was previously confirmed by Hüsken [34]. Here, the important observation for almost all amorphous nano silica samples that were analyzed is that the concentration needs to be less than 7% in order to obtain a mix that follows, as close as possible, a grading curve with $q=0.5$ (Fuller curve). By doing so, an expected minimum water demand is achieved. On the contrary, the PmS-6 presented a minimum distribution modulus of 0.30 to obtain reasonable results. In general, the smaller the particle size of the silica, less material is needed to find an optimum value for a fixed (q). It is important to notice that the optimization algorithm only takes into account the PSD of the non-reacted particles and does not consider effects caused by cement hydration or formation of water layers around the particles. This fact can explain why in almost all cases, the workability tests were not in concordance with the minimum calculated void faction.

A graphical analysis was made taking into account all fit coefficients (R^2). The R^2 values are plotted versus the respective distribution moduli (Fig. 12). Here, the maximum values of R^2 appeared for distribution moduli (q) in the range of 0.35 to 0.45. Confirming that, the best approximation to the target function of the composed granular mix, can be computed with a distribution modulus in the aforementioned range. This observation is in line with a (q) of 0.37 reported by Andreasen and Andersen [1], and 0.30 to 0.40 that were reported later by Hüsken [34]. One exception is the sample PmS-6, where the best approximation to the target function was computed when (q) had a minimum possible value.

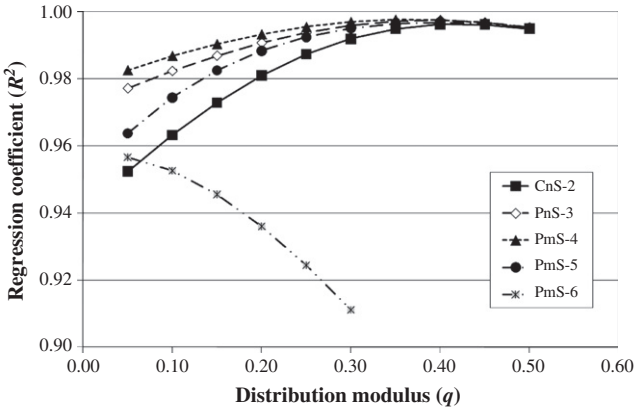

Fig. 12. Relation between the regression coefficients and the theoretical target line of different cement pastes containing amorphous nano silica.

7. Conclusions

In the present work, the mini spread-flow test for the determination of water demand, water film thickness and the impact on the workability of cement paste with amorphous nano silica are addressed. Different correlations have been derived which express these values in terms of granulometric properties and silica concentrations. Some of them are confirmed by literature, others are new. Several conclusions can be drawn and expressed as follows:

- Higher deformation coefficients (E_p) for amorphous silica with high content of nanoparticles were found which are bigger than that of cement. This indicates that water has a bigger influence on the workability of the hydrating system containing nano silica with high surface area.
- A linear relationship between the deformation coefficient and the specific surface area of nS/mS particles was confirmed. A similar thickness of the water layer of nS particles (24.8 nm), as reported by Hunger [31] for micron-sized powders, was confirmed and determined assuming a spherical particle shape. Taking into account the BET total and external specific surface area, a smaller water film was established. These values are helpful to calculate the water demand of a given silica sample with known specific surface area.
- In the experimental condition of the presented research, the addition of 0.5 to 4.0% (bwoc) nano silica to the cement paste can reduce the water demand without the use of superplasticizers. The concentration range found is related to distribution moduli (q) that are close to the Fuller curve to obtain a minimum water demand and void fraction in these types of granular mixes.
- Further research is required to modify the agglomerated state of the commercial nS in order to calculate a more accurate value of their computed specific surface area using LLD or DLS techniques. Even though the particle size ranges are comparable with the values obtained by SEM/STEM, a spherical shape and an amorphous structure are predominant in all samples.

Acknowledgments

This research was carried out under project number M81.1.09338 in the framework of the research program of the Materials innovation institute M2i. The authors wish also to express their thanks to Dr. J.W. Geus for his help in the SEM/STEM procedures and the following sponsors of the Building Materials research group: Bouwdienst Rijkswaterstaat, Graniet-Import Benelux, Kijlstra Betonmortel, Struyk Verwo, Attero, Enci, Provincie Overijssel, Rijkswaterstaat Directie Zeeland, A&G Maasvlakte, BTE, Alvon Bouwsystemen, V.d. Bosch Beton, Selor, Twee "R" Recycling, GMB, Schenk Concrete Consultancy, Intron, Geochem Research, Icopal, BN International, APP All Remove, Consensor, Eltomation, Knauf Gips, Hess ACC Systems and Kronos (chronological order of joining).

References

[1] A. Andreasen, J. Andersen, Über die Beziehung zwischen Kornabstufung und Zwischenraum in Produkten aus losen Körnern (mit einigen Experimenten), Kolloid-Zeitschrift 50 (1930) 217–228 (in German).

[2] A.M. Boddy, R.D. Hooton, M.D.A. Thomas, The effect of product form of silica fume on its ability to control alkali-silica reaction, Cem. Concr. Res. 30 (2000) 1139–1150.
[3] A. Bouvet, E. Ghorbel, R. Bennacer, The mini-conical slump flow test: analysis and numerical study, Cem. Concr. Res. 40 (2010) 1517–1523.
[4] J. Bjornstrom, A. Martinelli, A. Matic, L. Borjesson, I. Panas, Accelerating effects of colloidal nano silica for beneficial calcium-silicate-hydrate formation in cement, Chem. Phys. Lett. 392 (2004) 242–248.
[5] H.J.H. Brouwers, H.J. Radix, Self-compacting concrete: theoretical and experimental study, Cem. Concr. Res. 35 (2005) 2116–2136.
[6] J.S. Belkowitz, D. Armentrout, An investigation of nano silica in the cement hydration process, Proceeding 2010 Concrete Sustainability Conference, National Ready Mixed Concrete Association, U.S.A., 2010, pp. 1–15.
[7] S. Brunauer, P.H. Emmet, E. Teller, Adsortion of gases in multimolecular layers, J. Am. Chem. Soc. 62 (1938) 309–319.
[8] J. Byung-Wan, K. Chang-Hyun, T. Ghi-ho, P. Jong-Bin, Constr. Build. Mater. 21 (2007) 1351–1355.
[9] Cembureau, CEMBUREAU (The European Cement Association), www.cembureau.eu2008Brussels, Belgium.
[10] CEN EN 1015–3, Methods of test for mortar for masonry. Determination of consistence of fresh mortar (by flow table), European Commission for Standardization (CEN), 1999, pp. 1–10.
[11] CEN EN 196–1, Methods of testing cement part 1: determination of strength, European Commission for Standardization (CEN), 2005, pp. 1–36.
[12] CEN EN 197–1, Cement-part 1: composition and specifications and conformity criteria for common cements, European Commission for Standardization (CEN), 2000, pp. 1–33.
[13] M. Cyr, A. Tagnit-Hamou, Particle size distribution of fine powders by LASER diffraction spectroscopy. Case of cementitious materials, Mater. Struct. 34 (2001) 342–350.
[14] J.H. De Boer, B.C. Lippens, Studies in pore system in catalysts II. The shape of pores in aluminum oxides systems, J. Catal. 3 (1964) 38–43.
[15] F. De Larrard, Ultrafine particles for the making of very high strength concrete, Cem. Concr. Res. 19 (1989) 161–172.
[16] F. De Larrard, T. Sedran, Optimization of ultra-high-performance concrete by the use of a packing model, Cem. Concr. Res. 24 (6) (1994) 997–1009.
[17] S. Diamond, S. Sahu, Densified silica fume: particle sizes and dispersion in concrete, Mater. Struct. 39 (2006) 849–859.
[18] DIN EN 1097–7, Test for mechanical and physical properties of aggregates. Part 7: determination of particle density of filler—pyknometer method, German Institute of Normalization (DIN), 1999, p. 6.
[19] DIN ISO 9277, Determination of the Specific Surface Area of Solids by Gas Adsorption using the BET Method, German Institute of Normalization (DIN), 1995, pp. 1–19.
[20] P. Domone, Ch. Hsi-Wen, Testing of binder for high performance concrete, Cem. Concr. Res. 27 (8) (1997) 1141–1147.
[21] A. Dunster, Silica fume in concrete, Information Paper N° IP 5/09, IHS BRE Press, Garston, U.K., 2009, pp. 1–12.
[22] ENCI, Portland Cement CEM I, Heidelberg Cement Group, Brochure, May 2007, pp. 1–2.
[23] L.P. Esteves, On the hydration of water-entrained cement-silica systems: combined SEM, XRD and thermal analysis in cement pastes, Thermochim. Acta 518 (2011) 27–35.
[24] L.P. Esteves, P.B. Cachim, V.M. Ferreira, Effect of fine aggregate on the rheology properties of high performance cement-silica systems, Constr. Build. Mater. 24 (2010) 640–649.
[25] B. Friede, Microsilica-characterization of an unique additive, Proceedings of the 10th International Inorganic-Bonded Fiber Composites Conference (IIBCC 2006) — Sao Paulo, Brazil, Universidade de Sao Paulo and University of Idaho, October 15–18 2006, pp. 135–144.
[26] W.B. Fuller, S.E. Thompson, The laws of proportioning concrete, Trans. Am. Soc. Civ. Eng. 33 (1907) 222–298.
[27] J. Funk, D. Dinger, Predictive Process Control of Crowded Particulate Suspension Applied to Ceramic Manufacturing, Kluwer Academic Publishers, Boston, U.S.A., 1994, pp. 1–765.
[28] C. Furnas, The relation between specific volume, voids, and size composition in systems of broken solids of mixed sizes, Report 10, U.S. Bureau of Mines, 1928.
[29] W.D. Harkins, G. Jura, Surfaces of solids. XIII. A vapor adsorption method for the determination of the area of a solid without the assumption of a molecular area, and the areas occupied by nitrogen and other molecules on the surface of a solid, J. Am. Chem. Soc. 66 (8) (1944) 1366–1373.
[30] M. Hunger, H.J.H. Brouwers, Natural stone waste powders applied to SCC mix design, Restor. Build. Monum. 14 (2008) 131–140.
[31] M. Hunger, An Integral Design Concept for Ecological Self-Compacting Concrete, Ph.D. Thesis, Eindhoven University of Technology, The Netherlands, 2010, pp. 1–240.
[32] M. Hunger, H.J.H. Brouwers, Flow analysis of water-powder mixtures: application to specific surface area and shape factor, Cem. Concr. Compos. 31 (2009) 39–59.
[33] G. Hüsken, H.J.H. Brouwers, A new mix design concept for earth-moist concrete: a theoretical and experimental study, Cem. Concr. Res. 38 (2008) 1246–1259.
[34] G. Hüsken, A multifunctional design approach for sustainable concrete: with application to concrete mass products. Ph.D. Thesis, Eindhoven University of Technology, The Netherlands, 2010, pp. 1–243.
[35] ISO 13320–1, Particle Size Analysis – Laser Diffraction Methods – Part 1: General Principles, International Organization for Standardization, CH-1211 Genève 20, Switzerland, 1999, pp. 1–42.
[36] ISO 13321, Particle Size Analysis — Photon Correlation Spectroscopy, International Organization for Standardization, CH-1211 Genève 20, Switzerland, 2006, pp. 1–108.
[37] M. Jones, L. Zheng, M. Newlands, Comparison of particle packing models for proportioning concrete constituents for minimum voids ratio, Mater. Struct. 35 (249) (2002) 301–309.
[38] L.G. Li, A.K.H. Kwan, Mortar design based on water film thickness, Constr. Build. Mater. 25 (5) (May 2011) 2381–2390.
[39] D.F. Lin, K.L. Lin, W.C. Chang, H.L. Luo, M.Q. Cai, Improvements of nano-SiO_2 on sludge/fly ash mortar, Waste Manage. 28 (2008) 1081–1087.
[40] I. Marquardt, Determination of the composition of self-compacting concretes on the basis of the water requirements of the constituent materials, presentation of a new mix concept, Betonwerk+Fertigteiltechnik - BFT 11 (2002) 22–30.
[41] V. Marchuk, Dispersibility of the silica fume slurry in cement paste and mortar, Betontechnische Berichte Concrete Technology Reports 2001–2003, Verlag Bau +Technik, Düsseldorf, Germany, March 2004, pp. 125–132.
[42] T. Mangialardi, A.E. Paolini, Workability of superplasticized microsilica-portland cement concretes, Cem. Concr. Res. 18 (1988) 351–362.
[43] W. McCabe, J. Smith, Unit Operations of Chemical Engineering, McGraw-Hill Book Company, Inc., New York, U.S.A., 1956
[44] E.B. Nelson, D. Guillot, Cement additives and mechanism of action, Chapter 3, Well Cementing, second editions, Schlumberger ltd., Sugar Land, Texas, U.S.A., 2006, pp. 71–80.
[45] A.M. Neville, Properties of Concrete, 4th ed., Prentice Hall/Pearson, Harlow, U.K., 2000, pp. 1–844.
[46] H. Okamura, K. Ozawa, Mix-design for self-compacting concrete, Concr. Lib. Jpn. Soc. Civ. Eng. (JSCE) 25 (1995) 107–120.
[47] S. Palm, A. Wolter, Determining and optimizing the void filling of dry particle systems, Cem. Int. 7 (2009) 2–8.
[48] N.M. Plum, The predetermination of water requirement and optimum grading of concrete: under various conditions, Study N° 3, Report 96, The Danish National Institute of Building Research - Statens Byggeforskningsinstitut, Copenhagen, Denmark, 1950, pp. 1–96.
[49] J. Plank, Ch. Schroefl, M. Gruber, M. Lesti, R. Sieber, Effectiveness of polycarboxylate superplasticizers in ultra high strength concrete: the importance of PCE compatibility with silica fume, J. Adv. Concr. Technol. 7 (1) (2009) 5–12.
[50] Y. Qing, Z. Zenan, K. Deyu, Ch. Rongshen, Influence of nano-SiO_2 addition on properties of hardened cement paste as compared with silica fume, Constr. Build. Mater. 21 (2007) 539–545.
[51] G. Quercia, H.J.H. Brouwers, Application of nano-silica (nS) in concrete mixtures, in: Gregor Fisher, Mette Geiker, Ole Hededal, Lisbeth Ottosen, Henrik Stang (Eds.), 8th fib International Ph.D. Symposium in Civil Engineering. Lyngby, June 20–23, Denmark, 2010, pp. 431–436.
[52] H.W. Reinhardt, Beton als constructiemateriaal, Delftse Universitaire Pres., Delft, The Netherlands (in Dutch), 1998.
[53] G. Roddy, J. Chatterji, R. Cromwell, Well treatment composition and methods utilizing nano-particles, Halliburton Enery Services, United States of America Patent Application no 20080277116 A1, November 13 2008, pp. 1–12.
[54] L. Senff, D. Hotza, W.L. Repette, V.M. Ferreira, J.A. Labrincha, Mortars with nano-SiO_2 and micro-SiO_2 investigated by experimental design, Constr. Build. Mater. 24 (8) (2010) 1432–1437.
[55] L. Senff, J.A. Labrincha, V.M. Ferreira, D. Hotza, W.L. Repette, Effect of nano silica on rheology and fresh properties of cement pastes and mortars, Constr. Build. Mater. 23 (2009) 2487–2491.
[56] K. Sobolev, M. Ferrara, How nanotechnology can change the concrete world — part 1, Am. Ceram. Bull. 84 (10) (2005) 14–17.
[57] K. Sobolev, I. Flores, R. Hermosillo, Nanomaterials and nanotechnology for high-performance cement composites, Proceedings of ACI Session on Nanotechnology of Concrete: Recent Developments and Future Perspectives, November 7 2006, pp. 91–118, Denver, U.S.A.
[58] User manual, Zetasizer nanoseries, Malvern Instruments Ltd., U.K., 2007–2009, pp. 252–258.
[59] H. Vikan, H. Justnes, Rheology of cementitious paste with silica fume or limestones, Cem. Concr. Res. 37 (2007) 1512–1517.
[60] N. Vijayarethinam, Silica fume applications, World Cement, January 2009, pp. 97–100.
[61] www.malvern.comJuly 2010consulted.
[62] A.B. Yu, J. Bridgwater, A. Burbidge, On the modelling of the packing of fine particles, Powder Technol. 92 (1997) 185–194.

Abbreviations

A&A: Andreasen and Andersen
BET: Brunauer–Emmett–Teller method
DLS: Dynamic light scattering
EDS: X ray energy dispersive spectroscopy
ESEM: Environmental scanning electron microscopy
FEG: Field emission gun
LLD: Laser light diffraction
mS: Micro silica
nS: Nano silica
PSD: Particle size distribution
QELS: Quasi-elastic light scattering
SEM: Scanning electron microscopy

Sf: Silica fume
SS: Silica sand
SSA: Specific surface area [m^2/g] or [cm^2/cm^3]
STEM: Scanning transmission electron microscopy
t-plot: Statistical thickness method
CSH-gel: xCaO.ySiO$_2$.zH$_2$O gel

Roman

bwo: Based on the weight of cement [% m/m]
D: Particle or sphere diameter [nm], [μm] or [m]
D_0*:* Hägermann cone base diameter [cm]
D_i*:* Slump flow diameter i [cm]
$D_{i,arith.}^{i+1}$*:* Arithmetic mean of the particle size i [cm]
E_p*:* Deformation coefficient [−]
f_i*:* Volume fraction i [−]
M: Mass of particle or sphere [kg]
n: Total number of particle [−]
P: Adsorption pressure [mm Hg]
$P'(D)$*:* Particle grading function [% v/v]
P_0*:* Saturation vapor pressure [mmHg]
q: Distribution modulus [−]
$Q_{mix}(D_i)$*:* Composed mix function [% v/v]
$Q_{sol,k}$*:* Sieve residue solid k [% v/v]
$SSA_{BET,ext}$*:* External specific surface area (BET method) [m^2/g]
SSA_{Sph}*:* Sphere based computed specific surface area [m^2/g] [cm^2/cm^3]
$SSA_{BET,total}$*:* Total specific surface (BET method) [m^2/g]
V: Volume [cm^3]
$v_{sol,k}$*:* Volume of solid k [cm^3]
V_{total}*:* Total mix volume [cm^3]
V_w*:* Water volume [cm^3]
V_w/V_p*:* Volume based water-powder ratio [−]
w_i*:* Mass fraction i [−]
w/c: Water–cement ratio [−]

Greek

δ*:* Water film thickness [nm]
β_p*:* Water retention ratio or water demand [−]
Γ_p*:* Relative slump [−]
ξ*:* Particle shape factor [−]
ρ_s*:* Specific density [g/cm^3]
σ*:* Area covered by one molecule of adsorbate (N_2) [nm^2]
Ψ*:* Void fraction [−]

Subscripts

arith: Arithmetic
BET, ext: Brunauer–Emmett–Teller method external surface area
BET, total: Brunauer–Emmett–Teller method total surface area
i: Fraction index of the lower sieve, general counter
k: Counter variable for materials
max: Maximum
micro, max: Micropore maximum adsorption
min: Minimum
n: End value of the counter
p: Powder
S: Silica
s: solid
Sph: Sphere base
w: Water